

Deuteron photo-disintegration with polarised photons in the energy range 30 - 50 MeV

D. Babusci^a, V. Bellini^{b,c}, M. Capogni^{d,e}, L. Casano^d,
A. D'Angelo^d, F. Ghio^{f,g}, B. Girolami^{f,g}, D. Moricciani^{d,h},
C. Schaerf^{d,e}

^a*INFN - LNF, Via Enrico Fermi 40, I-00044 Frascati, Italy*

^b*Physics Department of the University of Catania, Corso Italia 57, I-95129 Catania, Italy*

^c*INFN - LNS, Viale S. Sofia 44, I-95125 Catania, Italy*

^d*INFN - Roma2, Via della Ricerca Scientifica 1, I-00133 Rome, Italy*

^e*Physics Department of the University of Rome "Tor Vergata", Via della Ricerca Scientifica 1, I-00133 Rome, Italy*

^f*Istituto Superiore di Sanità, Viale Regina Elena 299, I-00161 Rome, Italy*

^g*INFN - ISS, Viale Regina Elena 299, I-00161 Rome, Italy*

^h*Present Address: ISN, Avenue des Martyrs 53, F-38026 Grenoble Cedex, France*

Abstract

The reaction $d(\vec{\gamma}, np)$ has been studied using the tagged and polarised LADON gamma ray beam at an energy 30 – 50 MeV to investigate the existence of narrow dibaryonic resonances recently suggested from the experimental measurements in a different laboratory. The beam was obtained by Compton back-scattering of laser light on the electrons of the storage ring ADONE. Photo-neutron yields were measured at five neutron angle $\vartheta_n^{c.m.} = 22^\circ, 55.5^\circ, 90^\circ, 125^\circ$ and 157° in the center of mass system. Our results do not support the existence of such resonances.

PACS: 25.20 D, 24.70, 29.27 H

1 Introduction

The deuteron is the most fundamental nuclear laboratory and for this reason, deuteron photo-disintegration $d(\vec{\gamma}, np)$ has been extensively studied for the last sixty years [1]. The center of mass (c.m.) differential cross section for the reaction $d(\vec{\gamma}, n)p$ induced by linearly polarised gamma rays has been calculated, measured and discussed by several authors. We refer here to some extensive contributions only [2–4]. It can be written in the form:

$$\begin{aligned} \frac{d\sigma}{d\Omega}(E_\gamma, \vartheta_n, \varphi_n) &= I_0(E_\gamma, \vartheta_n) + PI_1(E_\gamma, \vartheta_n) \cos 2\varphi_n \\ &= I_0(E_\gamma, \vartheta_n) \left\{ 1 + P\Sigma(E_\gamma, \vartheta_n) \cos 2\varphi_n \right\} \end{aligned} \quad (1)$$

where ϑ_n is the angle between the neutron and photon momentum in the c.m. system and φ_n is the angle between the direction of the polarisation of the incoming photon and the reaction plane; P represents the degree of linear polarisation of the photon beam. The expression (1) is obtained only taking into account the spin of the photon. The microscopical structure of the $N - N$ interaction or the contribution of meson exchange currents (MEC) or the internal excitation of photo-disintegration configurations (IC), or the presence of sub-nucleonic degrees of freedom, influence only the form of the functions $I_0(E_\gamma, \vartheta_n)$ and $I_1(E_\gamma, \vartheta_n)$.

Recent experimental measurements of the deuteron photo-disintegration cross section made in Kharkov [5] with a linearly polarised photon beam obtained by coherent bremsstrahlung have shown some evidence of three narrow dibaryonic resonances in the differential cross section in the plane perpendicular to the beam polarisation $\varphi_n = 90^\circ$:

$$\frac{d\sigma}{d\Omega}(E_\gamma, \vartheta_n = 90^\circ, \varphi_n = 90^\circ) = I_0(E_\gamma, \vartheta_n = 90^\circ) - I_1(E_\gamma, \vartheta_n = 90^\circ) \quad (2)$$

they appeared at a very low excitation energies of the $(n-p)$ system as indicated in table 1 where we have shown the total energy of the $(n-p)$ system, the corresponding gamma ray energy and the apparent width:

Table 1

$E_{(n-p)}$ (MeV)	E_γ (MeV)	Γ (MeV)
1919.5	43.9	4.5
1933	57.4	2.7
1942	66.4	6.6

In figure 1 are shown the results obtained at Kharkov compared with the previous results obtained with the LADON beam [6]. The amazing result is that the Kharkov data are in good agreement with ours since their resonances are located between our points.

To verify the existence of the first and most impressive of these resonances we have taken advantage of the complete polarisation ($P \sim 1$) and good energy resolution of our tagged LADON beam $\sigma_{E_\gamma} \simeq 2 \text{ MeV}$ [7,8].

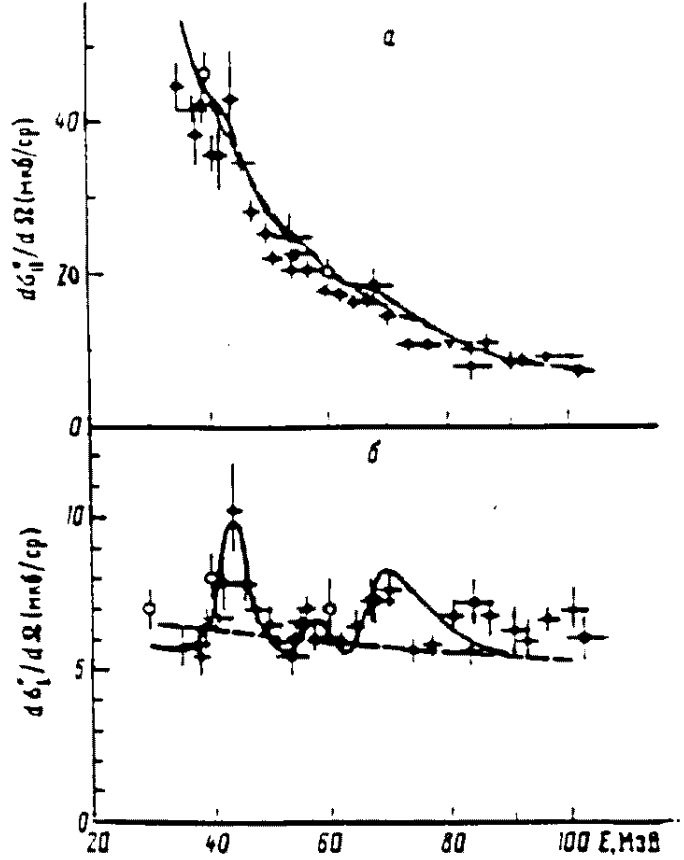


Fig. 1. $\left(\frac{d\sigma}{d\Omega}\right)_{\parallel,\perp}(E_\gamma, \vartheta_n = 90^\circ)$ from reference [5]; the symbol \circ shows the previous data obtained with the LADON beam [6]

2 Experimental Setup

2.1 The LADON $\vec{\gamma}$ beam

One of the most interesting features of the Compton backscattered $\vec{\gamma}$ ray beam is its polarisation: the $\vec{\gamma}$ rays emitted in the backward direction with energy close to the maximum have the same polarisation of the initial laser photons. Data were collected at different $\vec{\gamma}$ ray energies obtained by changing the incoming electron energy. The energy of the $\vec{\gamma}$ beam has been measured with an internal tagging detector where the scattered electrons are momentum analysed by one dipole and one quadrupole magnet of the ADONE storage ring lattice. The tagging system consists of a silicon solid-state μ -strip detector composed of 96 vertical strips with a pitch of $650 \mu m$, backed by a fast plastic scintillator.

The energy resolution of the $\vec{\gamma}$ beam depends on the energy of the scattered electron and the energy of the electrons circulating in the storage ring, but in any case we obtain $\sigma_{E_\gamma} \leq 2.2 \text{ MeV}$ [8]. During this experiment data are collected using different maximum energy of the $\vec{\gamma}$ beam $E_\gamma^{max} = 35, 38, 41, 45$ and 50 MeV in order to scan with high accuracy the energy region where the

first dibaryonic resonance is proposed.

The photon flux as been measured with a cylindrical *NaI* detector of 25.4 *cm* length and 25.4 *cm* diameter with an efficiency for photon detection of $\sim 100\%$.

2.2 Detectors

The target cell is an aluminium cylinder with a diameter of 3.81 *cm* full with deuterated liquid scintillator NE230 (full target) made of C_6D_6 . When a deuteron in the target disintegrates the proton does not have enough energy to leave the target and deposits all its energy into the target. The target is viewed by a photo-multiplier which provides a signal proportional to the energy deposited by the proton. The energy threshold used for this detector is 3 *MeV*, while the minimum energy for the proton coming from the deuteron photo-disintegration in our experimental condition is 12 *MeV*. For this reason we can reasonably assume a proton detection efficiency of $\sim 100\%$.

The neutrons escape the target and are detected by five time of flight (TOF) detectors made of horizontal cylinders, 30.4 *cm* of diameter and 15.4 *cm* of length, filled by organic liquid scintillator, NE213. These detectors are placed at a distance $D \simeq 60$ *cm* from the target and at angles $\vartheta_n = 22^\circ, 55.5^\circ, 90^\circ, 125^\circ$ and 157° . Each of them covers a solid angle of 0.13 *sr*. The threshold on the amplitude of the signal from these detectors is 0.5 *MeV*. The TOF between the proton pulse in the target and the neutron pulses are obtained with a resolution (FWHM) of $\Delta T \simeq 1.3$ *ns* (this value has been measured with the coincidence of the two γ photons emitted by a ^{60}Co source). Comparing the TOF of the neutrons (coming from the photo-nuclear reaction on the target) with that of the γ (Compton scattered in the target) detected in these counters we were able to have a reasonable measurement of the energy of the neutron by its TOF and to discriminate the neutrons against the e.m. background produced in the target. Calling $\tilde{t} = t_n - t_\gamma$ the TOF difference between a neutron and γ , the kinetic energy of the neutron is given by the following relation:

$$T_n = M_n c^2 \left(\sqrt{1 + \frac{D^2}{c^2 \tilde{t}^2 + 2Dc\tilde{t}}} - 1 \right). \quad (3)$$

To estimate the contribution of the background of events coming from the aluminium walls of the cell or the Carbon present in the full target we have also taken data with a second target (empty target) NE231 made of C_6H_6 , similar to the first one but with hydrogen instead of deuterium.

The experimental apparatus is shown in figure 2. Using this apparatus we have measured in coincidence the distribution of the protons pulses and the TOF of the neutrons emitted in the photo-reaction on the target.

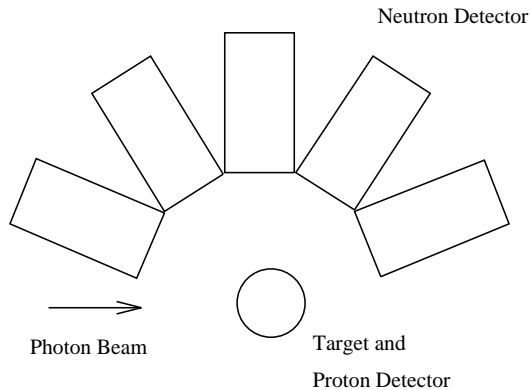


Fig. 2. Experimental apparatus

3 Data Analysis

The data analysis consists of two steps:

- 1) calibration of the apparatus, i.e. the tagging system, the active target for the proton detection, the neutron detectors and the estimation of their efficiencies;
- 2) selection of the $d(\vec{\gamma}, np)$ events and the calculation of the differential cross section;

The tagging system was calibrated using a magnetic pair spectrometer in coincidence, in our energy range the tagging energy calibration is linear as illustrated in [7,8] and its efficiency is $\varepsilon_{tag} = 0.96 \pm 0.03$.

The TOF calibration of the neutron detectors is determined by reference to the γ Compton diffused by the electrons in the target. The neutron detection efficiency was calculated using a Monte Carlo code [9] which takes into account all the nuclear reactions on the proton and carbon of the NE213 scintillators by the neutron coming from the deuteron photo-disintegration [10–13], and also experimental effects produced by the electronic chain, associated with each detectors, and the effect of the threshold used. A comparison between the experimental ADC spectra and the simulated one is shown in figure 3a), from this figure is derived the neutron detection efficiency which is quite constant as function of the neutron energy, as illustrated in figure 3b). From this we obtain its average value and its error $\langle \varepsilon_n(E_n) \rangle = (15.6 \pm 0.1)\%$.

The energy calibration of the active target is made using the kinematics of deuteron photo-disintegration, for which we know the energy of the incoming photon and the angle and energy of the outgoing neutron (in the LAB. system). We can use this information to determine the kinetic energy of the proton and comparing it with the ADC of the active target we derive its calibration.

The second step of the analysis which consists on the selection of the $d(\vec{\gamma}, np)$ events is also divided in two steps:

- 1) the rejection of the e.m. events due to Compton scattering in the target;
- 2) the identification of the $d(\vec{\gamma}, np)$ events, respect to other nuclear reaction coming from different reactions.

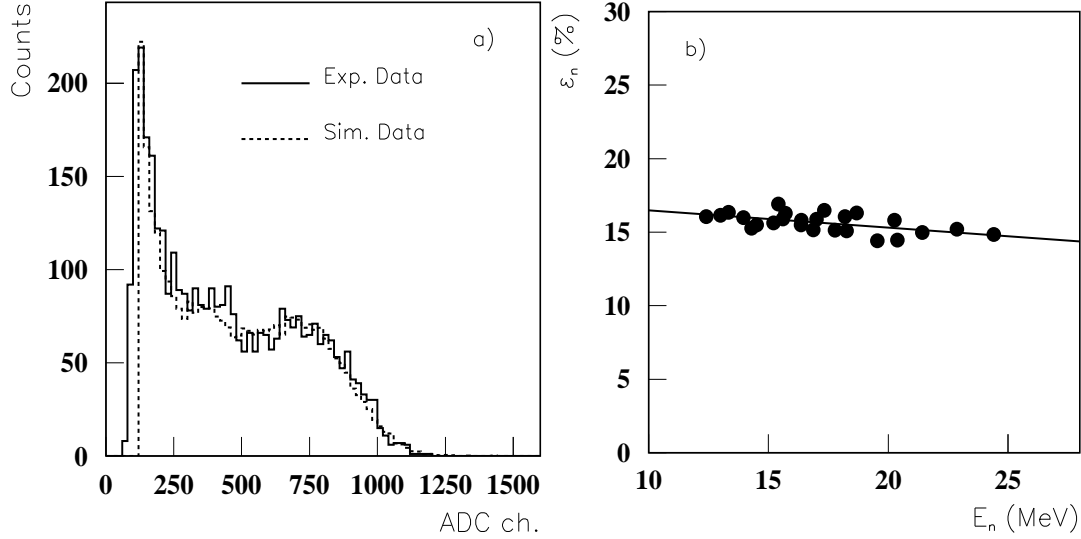


Fig. 3. a) Comparison between the experimental ADC spectra associated with the neutron detection and the ones simulated, b) Neutron efficiency as function of neutron energy

The rejection of the e.m. background was facilitated by the fact that in our target the form of the pulse associated with the detection of a hadron is different from that of an electron/photon, thus we have used the Head-Tail [14–18] technique. The Head is defined as the integral of the entire pulse, which is the signal which provides the energy of proton, while the Tail is the integral of the last part of it. This procedure allowed the separation of the nuclear events as shown in figure 4, where it is possible to recognise three types of events: *a)* the e.m. events, *b)* the nuclear events coming from the deuteron photo-disintegration and *c)* the nuclear events coming from photo-reaction on target walls or in the carbon also present in the target. The nuclear events *b)* and *c)* are clearly separated from those of type *a)* and we introduce a graphical cut on this plot to isolate them.

Further the identification of the nuclear events coming from reaction under study was done by a minimisation of the following variable:

$$\chi^2(E_\gamma, \vartheta_n, E_n, E_p) = \frac{(E_\gamma^{meas} - E_\gamma^{theo})^2}{\sigma_{E_\gamma}^2} + \frac{(\vartheta_n^{meas} - \vartheta_n^{theo})^2}{\sigma_{\vartheta_n}^2} + \frac{(E_n^{meas} - E_n^{theo})^2}{\sigma_{E_n}^2} + \frac{(E_p^{meas} - E_p^{theo})^2}{\sigma_{E_p}^2} \quad (4)$$

where the quantities with the superscript *meas* are those experimentally measured while the quantities with the superscript *theo* are calculated using the conservation of energy and momentum in our two body reaction. σ_{E_γ} , σ_{ϑ_n} , σ_{E_n} and σ_{E_p} are the uncertainties in the experimental quantities and are known with an error less than 20%. The reaction $d(\vec{\gamma}, np)$ is a two body one and its kinematics is completely determined if only the energy of the incoming photon E_γ and the angle of the outgoing neutron ϑ_n in the LAB. are known. For this rea-

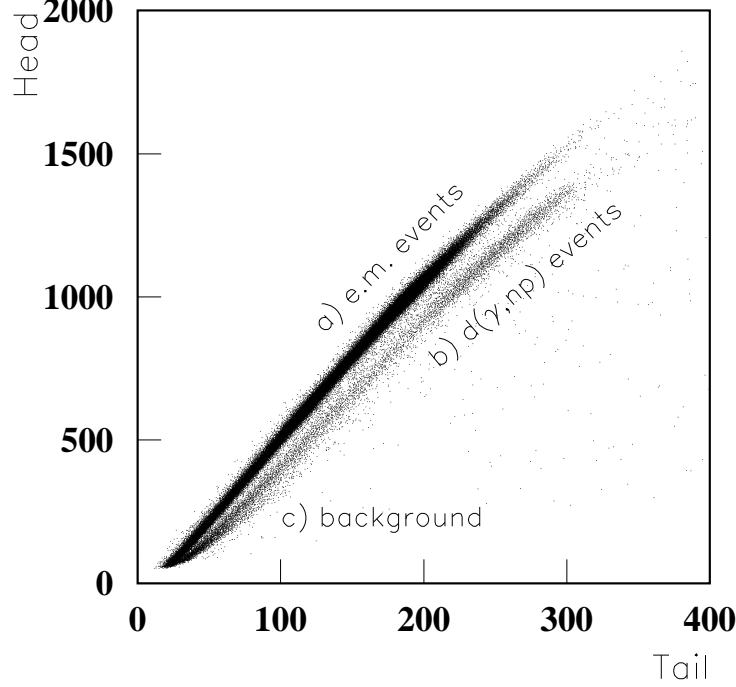


Fig. 4. Example of Head-Tail scatter plot from the active target data. For goods events the Head values must be proportional to the energy of proton emitted in the deuteron photo-disintegration. It must be greater then a given value which depend on the kinematics of the event and is around channel 700.

son in the minimisation procedure we use as independent variables these two, varying E_γ in the interval $(E_\gamma^{meas} - 3\sigma_{E_\gamma}, E_\gamma^{meas} + 3\sigma_{E_\gamma})$ and ϑ_n inside the solid angle covered by the neutron detector. The selection of the $d(\tilde{\gamma}, np)$ events can now be done using a cut in a combination of the dependent variables of the right-hand side of equation (4).

For each event we define the new variables $x_n = E_n^{theo} - E_n^{meas}$ and $x_p = E_p^{theo} - E_p^{meas}$. The distribution of $N(x_n, x_p)$ can be fitted by the following expression:

$$N(x_p, x_n) = Ae^{-\frac{(x_p - \mu_p)^2}{2\eta_p^2}} e^{-\frac{(x_n - \mu_n)^2}{2\eta_n^2}}, \quad (5)$$

and using the parameters A , μ_p , η_p , μ_n and η_n it is now possible to define a new variable: $z = \frac{(x_p - \mu_p)^2}{\eta_p^2} + \frac{(x_n - \mu_n)^2}{\eta_n^2}$ which follows a χ^2 distribution with two degrees of freedom: $\chi^2(z; 2) = \frac{exp(-z/2)}{2}$. The experimental distribution of z is shown in figure 5.

The excellent agreement between our data and the expression $A_\chi \chi^2(z; 2)$ for $z \leq z_{max} \simeq 3$ confirms the validity of this procedure. Studying the distribution of z for the three groups of events indicated in figure 4 we clearly see that the e.m. events coming from the class a) have $z > \sim 10$, the events coming from class b) have $z < \sim 3 - 3.5$ while the events of the class c) have $z > \sim 4$. In conclusion the number of events of deuteron photo-disintegration is given by

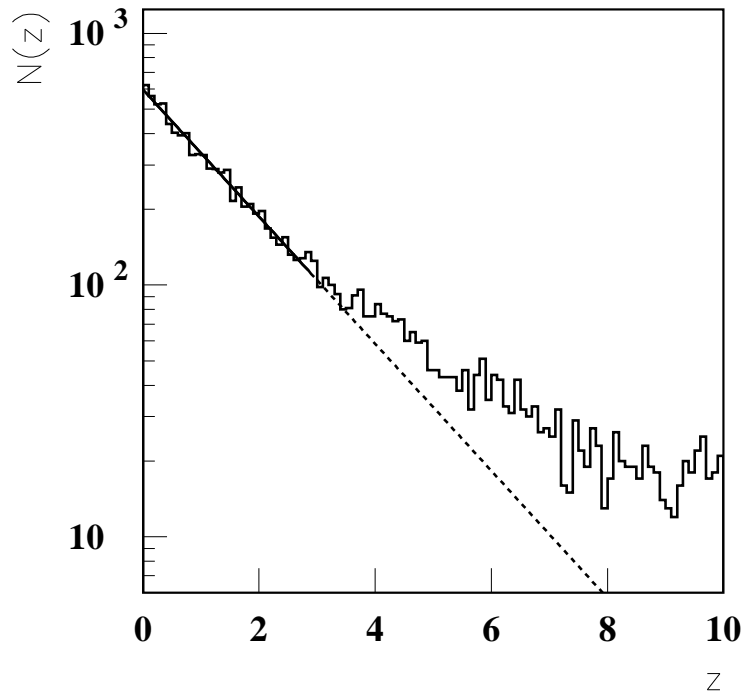


Fig. 5. Distribution of z for the full target events. The full line is a fit using the function $A_\chi \chi^2(z; 2)$ for $z < 3$ while the dashed line is its extrapolation for $z \in (3, 10)$.

the following relation:

$$N_{ev} = N_{ev}(z \leq z_{max}) + A_\chi \int_{z_{max}}^{\infty} \chi^2(z; 2) dz. \quad (6)$$

Where the first term is the number of events clearly identified while the second is an estimation of the good events mixed with the backgrounds. The second term is typically $2 \div 3\%$ of the first suggesting a systematic error in the estimate of the cross section of the order $\sim 1\%$. In figure 6 we have plotted the missing energy, $M.E. = E_\gamma - E_p - E_n$, in our reaction. For the events identified with this procedure ($z < \sim 3$) its average value is very close to the deuteron binding energy 2.2 MeV and the resolution is a few MeV . Its confirms that the result of our procedure is correct.

4 Experimental results and conclusion

The experimental cross section has been calculated according to:

$$\frac{d\sigma}{d\Omega} = \frac{N_{ev}}{N_\gamma L N_d \Delta\Omega_n \varepsilon_n} \quad (7)$$

where N_{ev} represent the nuclear events calculated with the procedure illustrated in the previous paragraph, N_γ is the number of incoming photons, L and N_d are the target length and density of scattering centres $N_d = \frac{N_{av}\rho}{A}$, $\Delta\Omega_n$

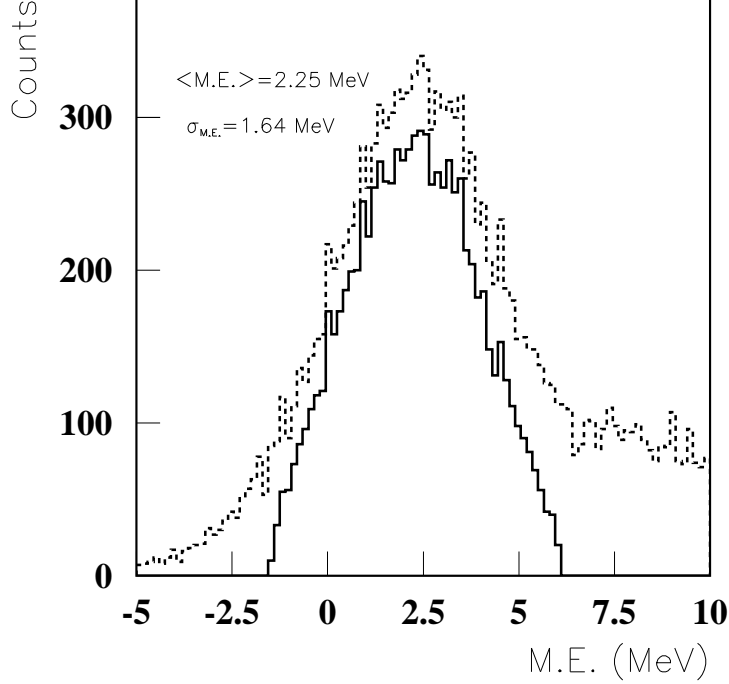


Fig. 6. Missing Energy for the reaction $d(\vec{\gamma}, np)$, dashed line all nuclear events(class b and c from the figure 4), full line events with the selection $z < 3$.

is the solid angle covered by the neutron detectors and ε_n is their efficiency. The factor $L\Delta\Omega_n$ is estimated using a Monte Carlo simulation which takes into account both the real dimensions of the intersection of the photon beam with the target and the neutron detectors size and distance from the target.

While we have taken data using different E_γ^{max} we have calculated the differential cross section at a given E_γ and $\vartheta_n^{c.m.}$ using different sets of data, this has been done in order to have a cross check of the entire procedure of analysis.

Our experimental data are shown in figures 7-11 where in each figure are illustrated the parallel cross section $d\sigma/d\Omega$, at $\varphi_n = 0^\circ$ the perpendicular cross section $d\sigma/d\Omega$ at $\varphi_n = 90^\circ$ and the asymmetry Σ for the five angles $\vartheta_n^{c.m.}$ as a function of the incoming $\vec{\gamma}$ -beam energy. The theoretical predictions which take into account One Body Current + Siegert + MEC + IC + Spin Orbit Current (full lines) are from the reference [19] we refer to this article for a discussion of the various aspects of the cross sections.

In figure 9 the first proposed dibaryon resonance of [5] is also shown (dashed line). A fluctuation of 3.3 standard deviation of the point around $44 MeV$ is necessary to make the two experiments compatible. The higher polarisation and lower background of the backscattered $\vec{\gamma}$ -ray give us greater confidence in the quality of our result.

5 Acknowledgments

We would like to thank W. Leidemann for the theoretical calculation of the cross section for the our energy and angular binning. We also would like to thank the technical staff of the LADON facility (E. Cima, M. Iannarelli, G. Nobili and E. Turri) for their essential contribution in obtaining a high-quality photon beam.

References

- [1] J. Chadwick and M. Goldhaber, *Nature* **134** (1934) 237;
- [2] H. Arenhövel, *Few-Body System* **4** (1988) 55;
- [3] F. Partovi, *Annals of Physics* **27** (1964) 79;
- [4] A. Cambi, B. Mosconi, P. Ricci, *Physical Review* **C26** (1982) 2358;
- [5] V.A. Ganenko, V.A. Gushin, U. V. Jetrovski, U. A. Kasatkin, L.I. Kolesnikov, S.E. Nagorny, V.D. Ofchignik, A.P. Rubaskin, P.V. Sorokin, A. A. Zaiaz, *Letters to JETP* **50** (1989) 220;
- [6] M.P. De Pascale, G. Giordano, G. Matone, D. Babusci, R. Bernabei, O.M. Bilianuk, L. Casano, S. d'Angelo, M. Mattioli, P. Picozza, D. Prospero, C. Schaerf, S. Frullani, B. Girolami, *Physical Review* **C32** (1985) 1830;
- [7] D. Babusci, E. Cima, M. Iannarelli, E. Turri, F. Basti, I. Halpern, L. Casano, A. D'Angelo, D. Moricciani, P.G. Picozza, C. Schaerf, B. Girolami, *Nuclear Instruments and Methods* **305**, (1991), 19;
- [8] D. Babusci, V. Bellini, M. Capogni, L. Casano, A. D'Angelo, F. Ghio, B. Girolami, L. Hu, D. Moricciani and C. Schaerf, "Polarized and tagged gamma-rays LADON beams", *La Rivista del Nuovo Cimento*, 19 5 (1996);
- [9] Anghinolfi A., Ricco G., Corvisiero P., Masulli F. *Nuclear Instruments and Methods* **165**, (1979), 217;
- [10] W. N. Hess, *Review of Modern Physics*, **30** (1958) 368;
- [11] V. T. McLane et al., **Neutron Cross Section** Vol. **2** (1982) Ed. Academic Press;
- [12] A. Dal Guerra, *Nuclear Instruments and Method*, **135** (1976) 337;
- [13] *Symposium on neutron cross section for 10 to 50 MeV*, **BNL-NCS-51245**, Vol. 1 e 2, (1980) Edited by M.R. Bhat and S. Pearlstein;
- [14] P.G. Sjölin, *Nuclear Instruments and Method* **37** (1965) 45;
- [15] Birks *The Theory and practice of scintillation counting* Ed. Pergamon, London, 1964;

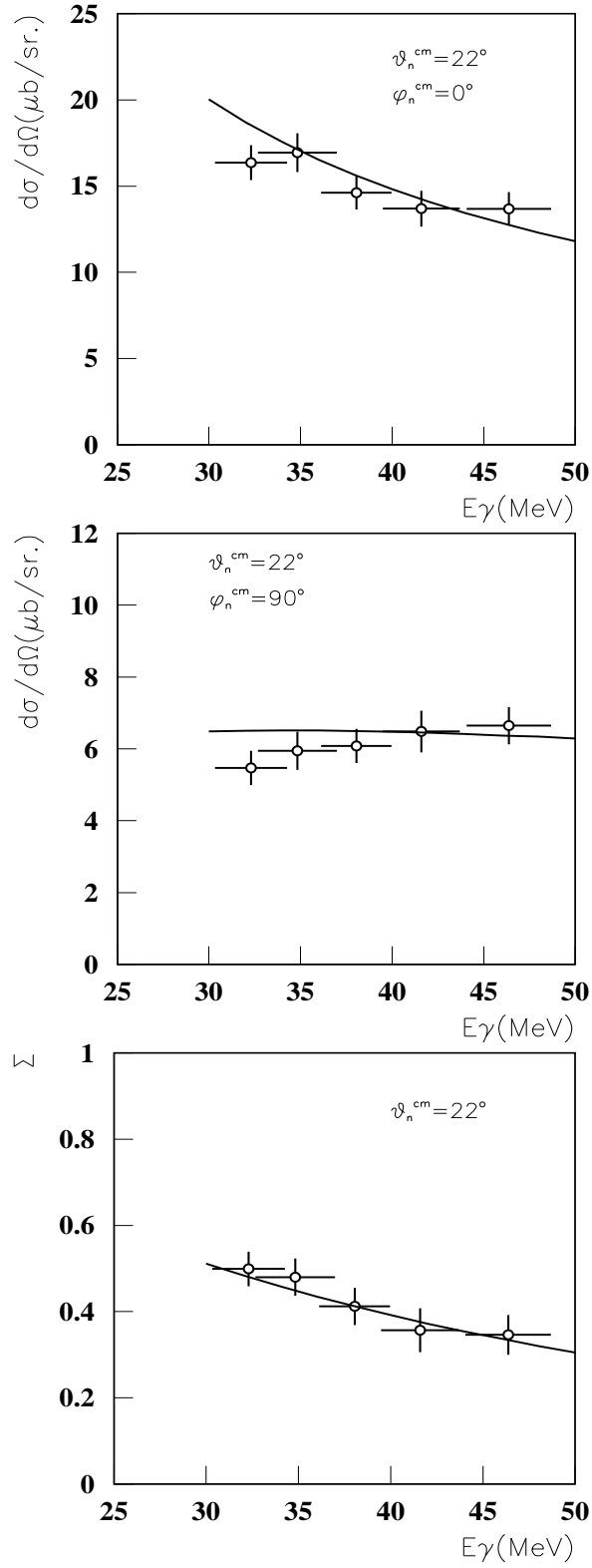


Fig. 7. Parallel, Perpendicular cross section and Asymmetry for $\vartheta_n^{c.m.} = 22^\circ$

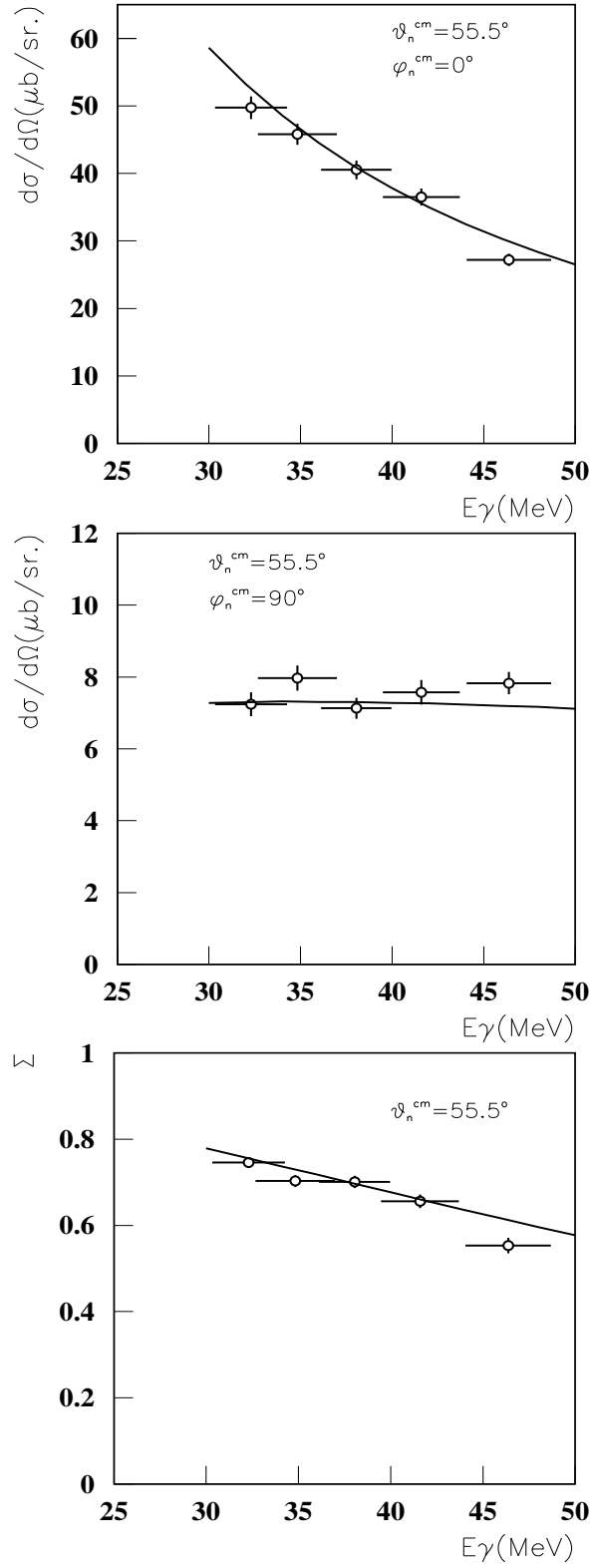


Fig. 8. Parallel, Perpendicular cross section and Asymmetry for $\vartheta_n^{c.m.} = 55.5^\circ$

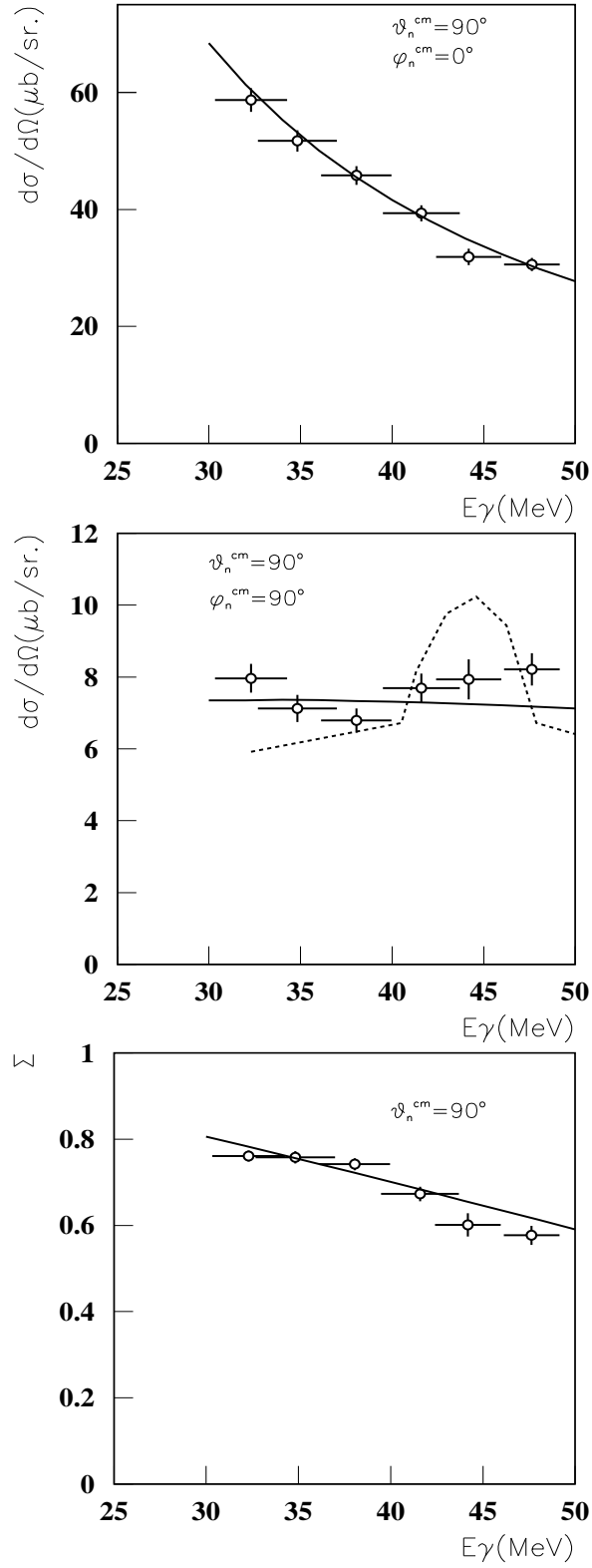


Fig. 9. Parallel, Perpendicular cross section and Asymmetry for $\vartheta_n^{c.m.} = 90^\circ$

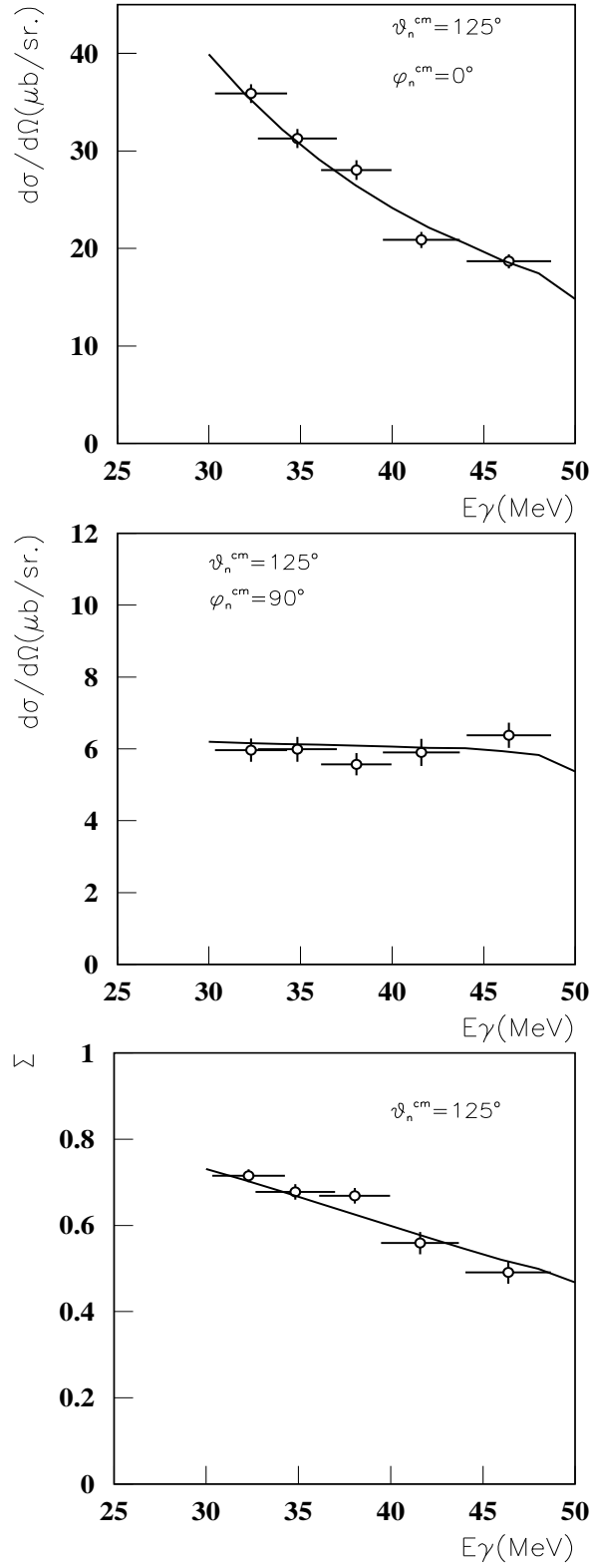


Fig. 10. Parallel, Perpendicular cross section and Asymmetry for $\vartheta_n^{c.m.} = 125^\circ$

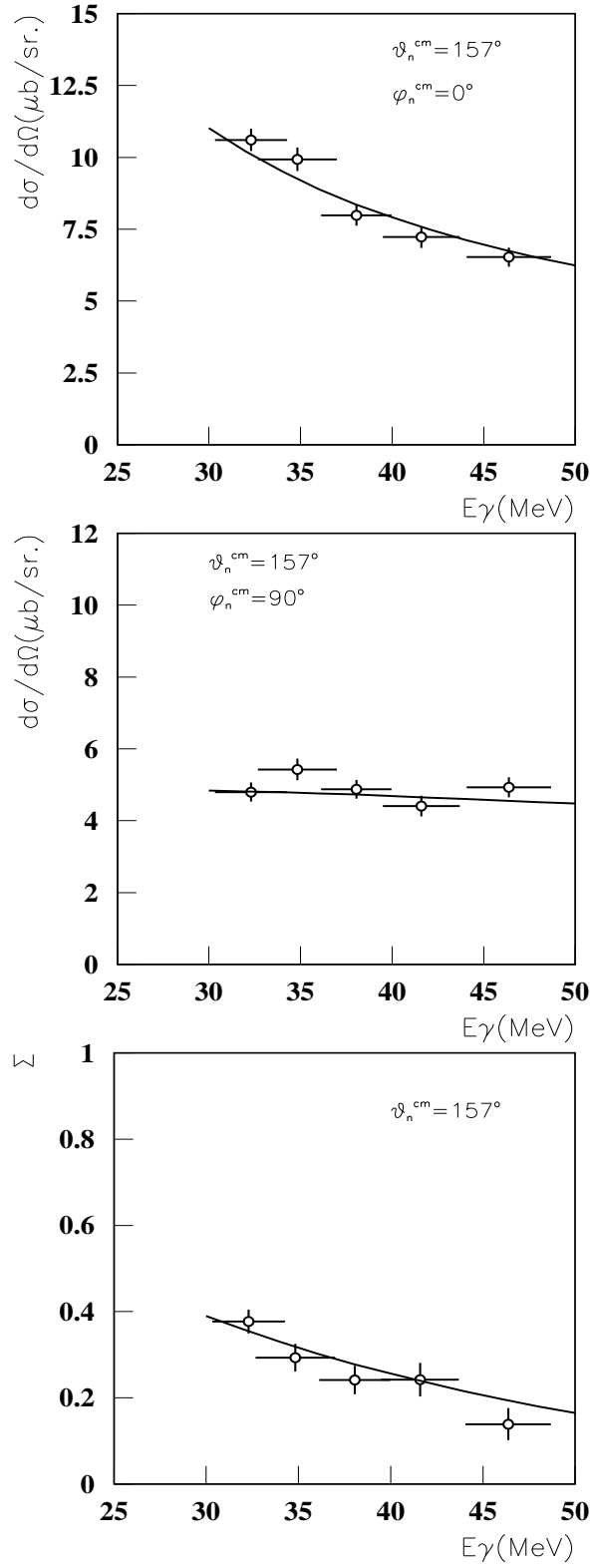


Fig. 11. Parallel, Perpendicular cross section and Asymmetry for $\vartheta_n^{c.m.} = 157^\circ$

- [16] R. Owen *IRE Transactions on Nuclear Science*, **5** (1958) 198;
- [17] F. Kuchnir, J. Lynch, *IEEE Transactions on Nuclear Science*, **NS-3** (1968) 107;
- [18] F.D. Brooks, *Nuclear Instruments and Methods* **4** (1959) 151;
- [19] P. Wilhelm, W.Leidemann, H.Arenhövel, *Few-Body Syst.* **3** (1988) 111;